



ELSEVIER

Contents lists available at ScienceDirect

NeuroImage: Clinical

journal homepage: www.elsevier.com/locate/ynicl

MR diffusion changes in the perimeter of the lateral ventricles demonstrate periventricular injury in post-hemorrhagic hydrocephalus of prematurity

Albert M. Isaacs^{a,b,*}, Christopher D. Smyser^{c,d,e}, Rachel E. Lean^f, Dimitrios Alexopoulos^d, Rowland H. Han^g, Jeffrey J. Neil^d, Sophia A. Zimbalist^g, Cynthia E. Rogers^{e,f}, Yan Yan^h, Joshua S. Shimony^c, David D. Limbrick Jr.^{e,g}

^a Department of Biology and Biomedical Sciences, Washington University in St. Louis, St. Louis, MO, United States

^b Department of Clinical Neurosciences, University of Calgary, Calgary, Alberta, Canada

^c Mallinckrodt Institute of Radiology, Washington University School of Medicine, St. Louis, MO, United States

^d Department of Neurology, Washington University School of Medicine, St. Louis, MO, United States

^e Department of Pediatrics, Washington University School of Medicine, St. Louis, MO, United States

^f Department of Psychiatry, Washington University School of Medicine, St. Louis, MO, United States

^g Department of Neurosurgery, Washington University School of Medicine, St. Louis, MO, United States

^h Department of Surgery, Washington University School of Medicine, St. Louis, MO, United States

ARTICLE INFO

Keywords:

Intraventricular hemorrhage
Periventricular white matter
Subventricular zone
Ventricular zone

ABSTRACT

Objectives: Injury to the preterm lateral ventricular perimeter (LVP), which contains the neural stem cells responsible for brain development, may contribute to the neurological sequelae of intraventricular hemorrhage (IVH) and post-hemorrhagic hydrocephalus of prematurity (PHH). This study utilizes diffusion MRI (dMRI) to characterize the microstructural effects of IVH/PHH on the LVP and segmented frontal-occipital horn perimeters (FOHP).

Study design: Prospective study of 56 full-term infants, 72 very preterm infants without brain injury (VPT), 17 VPT infants with high-grade IVH without hydrocephalus (HG-IVH), and 13 VPT infants with PHH who underwent dMRI at term equivalent. LVP and FOHP dMRI measures and ventricular size-dMRI correlations were assessed.

Results: In the LVP, PHH had consistently lower FA and higher MD and RD than FT and VPT ($p < .050$). However, while PHH FA was lower, and PHH RD was higher than their respective HG-IVH measures ($p < .050$), the MD and AD values did not differ. In the FOHP, PHH infants had lower FA and higher RD than FT and VPT ($p < .010$), and a lower FA than the HG-IVH group ($p < .001$). While the magnitude of AD in both the LVP and FOHP were consistently less in the PHH group on pairwise comparisons to the other groups, the differences were not significant ($p > .050$). Ventricular size correlated negatively with FA, and positively with MD and RD ($p < .001$) in both the LVP and FOHP. In the PHH group, FA was lower in the FOHP than in the LVP, which was contrary to the observed findings in the healthy infants ($p < .001$). Nevertheless, there were no regional differences in AD, MD, and RD in the PHH group.

Conclusion: HG-IVH and PHH results in aberrant LVP/FOHP microstructure, with prominent abnormalities

Abbreviations: AD, axial diffusivity; CSF, cerebrospinal fluid; dMRI, diffusion MRI; HG-IVH, high-grade intraventricular hemorrhage; IVH, intraventricular hemorrhage; FA, fractional anisotropy; FOHP, frontal and occipital horn perimeter; FT, full term; LVP, lateral ventricular perimeter; MD, mean diffusivity; PHH, post hemorrhagic hydrocephalus; RD, radial diffusivity; VPT, very preterm

Funding: This work was supported by the Vanier Canada Graduate Scholarship [grant number 396212]; National Institutes of Health [grant numbers K02 NS089852, K23 NS075151, K23 MH105179, TL1 TR002344, P30 NS098577, R01 MH113570, R01 HD061619, and R01 HD057098]; Child Neurology Foundation; Cerebral Palsy International Research Foundation; The Dana Foundation; March of Dimes Prematurity Research Center at Washington University; The Doris Duke Charitable Foundation; and the Eunice Kennedy Shriver National Institute of Child Health & Human Development of the National Institutes of Health [grant number U54 HD087011]. None of the organizations listed had any role in the study design, data collection, data analysis, data interpretation, writing or decision to submit the report for publication.

Declaration of Competing Interest: Dr. Limbrick receives research funds and/or research equipment for unrelated projects from Medtronic, Inc., Karl Storz, Inc., and Microbot Medical, Inc. Dr. Limbrick has received philanthropic equipment contributions for humanitarian relief work from Karl Storz, Inc. and Aesculap, Inc. The authors have no personal, financial, or institutional interest in any of the materials, or devices described in this article.

* Corresponding author at: Washington University School of Medicine, 660 Euclid Ave, St. Louis, MO 63110, United States.

E-mail address: albert.isaacs@wustl.edu (A.M. Isaacs).

<https://doi.org/10.1016/j.nicl.2019.102031>

Received 21 April 2019; Received in revised form 1 October 2019; Accepted 4 October 2019

Available online 08 October 2019

2213-1582/ © 2019 The Authors. Published by Elsevier Inc. This is an open access article under the CC BY-NC-ND license

(<http://creativecommons.org/licenses/by-nc-nd/4.0/>).

among the PHH group, most notably in the FOHP. Larger ventricular size was associated with greater magnitude of abnormality. LVP/FOHP dMRI measures may provide valuable biomarkers for future studies directed at improving the management and neurological outcomes of IVH/PHH.

1. Introduction

Very preterm birth (delivery prior to 32 weeks gestation) is a major cause of neonatal morbidity and mortality worldwide. (Liu et al., 2016; Stoll et al., 2015) Unfortunately, up to 40% of these infants sustain intracranial hemorrhage within their germinal matrix, (Stoll et al., 2015) a periventricular region where the neural stem cells for cortical development reside. (Brat, 2010; du Plessis, 2009) Commonly, germinal matrix hemorrhage extends into the cerebral ventricles to cause intraventricular hemorrhage (IVH, Inder et al., 2018, Mukerji et al., 2015) which is classified into four grades of severity. (Inder et al., 2018; Papile et al., 1978) Grades I and II are considered 'low-grade', associated with neuromotor impairment in up to 33% of affected infants (Ancel et al., 2006; Sherlock et al., 2005) and carry a two-fold risk of poor cognitive outcomes. (Patra et al., 2006) Grades III and IV are classified as 'high-grade' and have even poorer neurological outcomes, with neuromotor and cognitive deficits in over 90% of affected infants. (Klebermass-Schrehof et al., 2012) Further, approximately one-third of preterm infants who sustain high-grade hemorrhage progress to develop post-hemorrhagic hydrocephalus (PHH, Adams-Chapman et al., 2008) which is characterized by cerebrospinal fluid (CSF) accumulation within the ventricles and raised intracranial pressure. (Kahle et al., 2016) PHH confers even more risk for neurological impairment and typically requires neurosurgical CSF diversion. (Adams-Chapman et al., 2008; Kahle et al., 2016; Robinson, 2012).

While advances in the care of infants with IVH/PHH have been made, their neurological outcomes remain poor, due in part to a limited understanding of the pathophysiology of the disease. (Koschnitzky et al., 2018; McAllister et al., 2015) However, mounting evidence has directed focus to the neurogenic region along the lateral ventricular perimeter (LVP, Bystron et al., 2008, Castaneyra-Ruiz et al., 2018, Jimenez et al., 2009, McAllister et al., 2017) given its critical role in neurodevelopment and function as a CSF-brain barrier. (Bystron et al., 2008; Dominguez-Pinos et al., 2005; Gotz and Huttner, 2005) The LVP comprises the ventricular and subjacent subventricular zones, which house progenitor cells that differentiate into cortical neurons and neuroglia, and is juxtaposed by periventricular white matter fibers that are medial to larger bundle tracts such as the corpus callosum, optic radiations and internal capsules. (Gotz and Huttner, 2005) The structure and cellular processes in the LVP may be severely impaired by IVH, (Inder et al., 2018; McAllister et al., 2017) which compromises its CSF-brain barrier function and exposes the periventricular white matter to injurious mechanisms and CSF toxins. (Alvarez and Teale, 2007; Mishra and Teale, 2012) Indeed, there is histopathological evidence of severe LVP and periventricular white matter damage in infants with IVH/PHH and other forms of hydrocephalus. (Dominguez-Pinos et al., 2005; Jimenez et al., 2009; McAllister et al., 2017) Further, on conventional MRI, the LVP and periventricular white matter commonly demonstrate T₂W hyperintensity in infants with IVH/PHH, most notably in the frontal and occipital horn perimeter regions (FOHP), which may be associated with hypoxic-ischemic injury and/or trans-ependymal edema. (Ho et al., 2012; Segev et al., 2001).

Diffusion MRI (dMRI) techniques, such as diffusion tensor imaging (DTI), delineate microstructural changes in white matter by measuring water diffusion anisotropy. (Neil et al., 1998; Pierpaoli et al., 1996) dMRI has been used to characterize the effects of IVH and other forms of hydrocephalus on periventricular white matter integrity (Buckley et al., 2012; Mangano et al., 2016; Yuan et al., 2012; Yuan et al., 2013). Specifically, dMRI parameters, including fractional anisotropy (FA), axial diffusivity (AD), radial diffusivity (RD) and mean diffusivity (MD), have been shown to correlate with

neurodevelopmental outcomes in neonates with aqueductal stenosis and other congenital and obstructive forms of hydrocephalus (Buckley et al., 2012; Mangano et al., 2016; Yuan et al., 2013), and have been shown to improve following hydrocephalus treatment (Buckley et al., 2012; Mangano et al., 2016; Scheel et al., 2012). However, the existing dMRI literature for IVH/PHH has focused on large bundle periventricular white matter fibers such as the corpus callosum and internal capsule, which are anatomically and developmentally distinct from the LVP (Assaf et al., 2006; Mangano et al., 2016; Scheel et al., 2012; Yuan et al., 2010; Yuan et al., 2012; Yuan et al., 2013). The LVP has not been examined with dMRI across populations primarily because it is a difficult region to study due to volume averaging effects at the margin of the ventricle. Furthermore, while correlations between ventricular size and large bundle periventricular white matter dMRI measures have been informative in other forms of hydrocephalus (Akbari et al., 2015; Cauley and Cataltepe, 2014), the relationships between ventricular size and LVP tissue integrity in IVH/PHH have not been studied.

Utilizing dMRI to define the effects of IVH/PHH on the LVP, and in particular the neural stem cell rich FOHP, may provide insights into the deleterious effects of IVH/PHH on ependymal CSF-brain barrier function and periventricular white matter integrity, affording a foundation for future studies of therapeutic interventions which address those effects. In addition, assessing the relationships between dMRI measures and ventricular size will not only add to our understanding of IVH/PHH pathophysiology, but may help define the role of therapeutic ventricular decompression in PHH and guide clinical decision-making regarding the timing for CSF diversion surgery. To address these questions, this study leverages a large prospective cohort of very preterm infants with/without IVH/PHH and full-term healthy control infants in order to: 1) assess the effects of IVH/PHH on LVP and FOHP regions; and 2) define the relationships between ventricular size and LVP/FOHP dMRI measures. We hypothesized that preterm infants with IVH/PHH will demonstrate aberrant dMRI microstructural measures of the LVP/FOHP when compared to uninjured preterm and full-term controls, and that dMRI measures will correlate with linear indices of ventricular size, with larger ventricles correlating with greater abnormalities in dMRI measures.

2. Methods

2.1. Subjects

Four groups of prospectively recruited infants were assessed between May 2007 and August 2016. The first group, the very preterm group (VPT), included infants born ≤ 30 weeks gestational age with no or low-grade IVH. The second group, the high-grade intraventricular hemorrhage group (HG-IVH), was comprised of age-matched VPT infants who developed grade III/IV IVH identified on cranial ultrasound within the first month of life. The third group, the post-hemorrhagic hydrocephalus group (PHH), was comprised of VPT infants who sustained grade III/IV IVH identified on cranial ultrasound within the first month of life and required neurosurgical treatment for hydrocephalus. Well-established Hydrocephalus Clinical Research Network criteria were applied for the diagnosis of PHH and the timing of neurosurgical treatment (Wellons et al., 2017), which included a reservoir or sub-galeal shunt placement for temporary ventricular access, or permanent treatment with endoscopic third ventriculostomy (ETV) or ventriculoperitoneal (VP) shunt. All VPT, HG-IVH and PHH infants were recruited from a Level-III Neonatal Intensive Care unit at a large regional hospital. The fourth group comprised of healthy full-term (FT) infants who were born

at 38–42 weeks gestational age. FT infants were identified from a larger cohort who were undergoing neonatal neuroimaging scans as part of an existing contemporaneous fetal monitoring study conducted at an adjoining maternity hospital. To ensure the FT group had no confounding health issues at birth, additional exclusion criteria included acidosis ($\text{pH} < 7.20$) on cord blood gas or blood gas obtained during the first hour of life or evidence of *in utero* illicit substance exposure. Exclusion criteria for all four groups included inability to obtain informed consent from an infant's parent, presence of chromosomal abnormalities and/or proven congenital infections (e.g., cytomegalovirus, toxoplasma, rubella). As shown in Supplementary Figure 1, a total of 206 infants (FT=76, VPT=91, HG-IVH=20, PHH=19) with DTI data were screened for possible inclusion in the study. Reasons for study exclusion across the groups included: acidosis (FT=8), positive maternal urine drug screen (FT=5, VPT=1, HG-IVH=1), and atypical pattern of brain injury/abnormal MRI finding (FT=2, VPT=2).

Written informed consent was obtained from at least one parent of every infant. Institutional Review Board approval for this study was obtained from the Washington University Human Research Protection office.

2.2. Clinical variables

To account for differences in medical status between groups, perinatal clinical information obtained for each infant was used to calculate their clinical risk index score. (Rogers et al., 2016) The presence or absence of each of 10 factors were scored as 1 or 0 respectively. There were 9 patient-related factors, which included: 1) small for gestational age at birth or intrauterine growth restriction; 2) received oxygen therapy at 36 weeks; 3) received postnatal steroids; 4) developed necrotizing enterocolitis; 5) had a patent ductus arteriosus requiring indomethacin or ibuprofen therapy; 6) had retinopathy of prematurity; 7) developed culture-positive neonatal sepsis; 8) weight-for-height/length ratio at the time of term equivalent MRI acquisition > 3 standard deviations below the measured ratio at birth; and 9) duration receiving total parenteral nutrition above the 75th percentile. A point was also scored if the mother did not receive antenatal steroids. All scores were collated to obtain a composite risk index score on a Likert scale of 10 - the higher the score, the poorer the presumed neonatal health (Rogers et al., 2016).

2.3. Image acquisition

VPT, HG-IVH and PHH infants underwent an MRI scan at/near term equivalent age (35–43 weeks postmenstrual age). FT infants were scanned

within the first four days of birth. All 13 PHH infants had undergone reservoir placement prior to their study MRI, with 6 of these infants also undergoing shunt placement prior to their MRI scan. However, due to the small group sizes, we were not powered to analyze for potential effects of permanent shunt placement. Following well-described institutional neonatal imaging practices (Mathur et al., 2008), all infants were imaged without sedation during natural sleep or while resting quietly. MRI images were acquired in a 3T Siemens Trio system (Siemens Medical Solutions, Erlangen, Germany) using an infant-specific, quadrature head coil (Advanced Imaging Research, Cleveland, OH, USA). Anatomical images included a T₁W sagittal, magnetization-prepared rapid gradient echo sequence (repetition time 1550 ms, inversion time 1100 ms, echo time 3.05 ms, flip angle 15°, $1 \times 1 \times 1.25 \text{ mm}^3$ voxels); T₂W fast spin echo sequence (repetition time 8210 ms, echo time 161 ms, $1 \times 1 \times 1 \text{ mm}^3$ voxels); and DWI sequence (repetition time 13300 ms, echo time 112 ms, $1.2 \times 1.2 \times 1.2 \text{ mm}^3$ voxels, 31 to 48 b-directions with amplitudes ranging from 0 to 1200 s/mm²).

2.4. Image processing

The diffusion signal attenuation curve was modeled as a mono-exponential function plus a constant, and diffusion parameters were estimated using Bayesian Probability Theory (Kroenke et al., 2006). FA, AD, RD and MD maps were generated from the dMRI slices. Principal eigenvector maps were generated with DSI studio software (<http://dsi-studio.labsolver.org>). Periventricular regions of interest (ROI) were generated using MATLAB version 9.2 (MathWorks, Natick, MA, USA) and semi-automated segmentation scripts. Briefly, numerical thresholds were applied to MD maps to isolate the lateral ventricles as being central structures with high MD values. The ventricles areas were dilated, and a subtraction operation isolated the periventricular areas. Subsequent analyses of the lateral ventricles focused on the entire circumference of the periventricular area (LVP; Fig. 1 top row) or segmented Frontal and Occipital Horn Perimeters (FOHP; Fig bottom row). Both regions were identified on 3 contiguous axial slices in order to minimize through-slice partial volume averaging. Infants with porencephalic cysts were able to be processed using standard procedures. Additional DTI data loss was attributed to poor scan quality/motion artifacts ($n = 20$) and severe brain injury (PHH, $n = 2$). However, those with severe white matter cysts causing significant changes in ventricular morphology near the foramen of Monro were not included in the study (VPT, $n = 7$).

Consistency of the algorithm was tested by performing intra-subject comparisons and the same dMRI values were consistently obtained

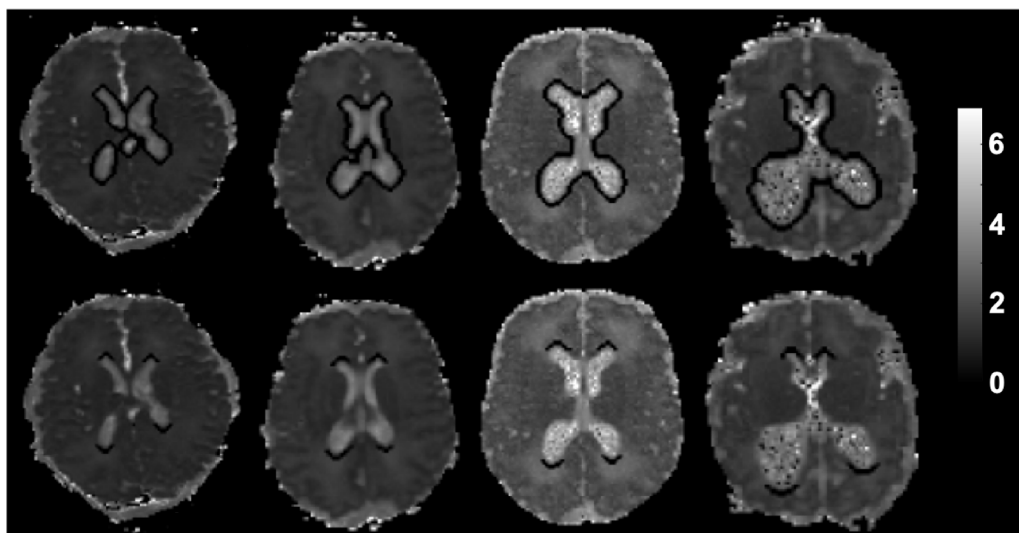


Fig. 1. Segmentation of ROIs: Representative contiguous axial mean diffusivity maps of infants with variable ventricular morphologies demonstrating segmentation of the lateral ventricular perimeter (top row) and frontal and occipital horn perimeter (bottom row).

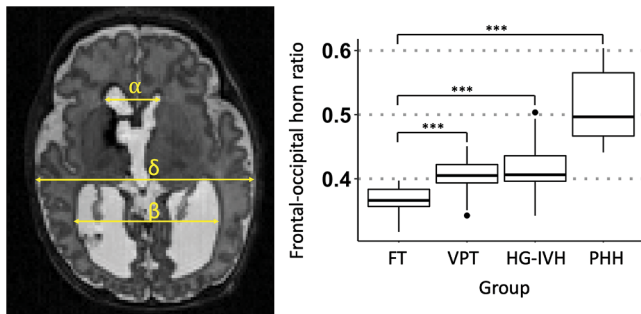


Fig. 2. Linear ventricular size measurement: Representative axial T₂WI of a very preterm infant with post-hemorrhagic hydrocephalus (PHH). Ventricular size was determined by the frontal and occipital horn ratio which was calculated as $(\alpha + \beta)/2\delta$. The Box and whisker diagram demonstrates PHH group had the largest ventricular size among 158 infants ($p < 0.001$, ***). There was no difference in ventricular size between the VPT and HG-IVH infants, although both groups had median ventricular sizes that were larger than that of the FT control infants.

across each iteration. To further validate the algorithm, measures from the algorithm were compared to those obtained from manually defined ROIs placed in the lateral ventricular perimeter across all four groups by a single expert rater (D.A.). dMRI measures generated using both manual and automated approaches were strongly correlated across groups ($r = 0.89 - 0.91$, $p < .001$).

Ventricular size was measured by an expert single rater (S.A.Z) on axial T₂W image using the frontal-occipital horn ratio approach (O’Hayon et al., 1998), which sums the distance between the widest lateral walls of the frontal and occipital horns, divided by twice the widest biparietal diameter at the level of the foramen of Monro (Fig. 2). Reproducibility of these measures was established across groups using measurements made by an independent rater (D.A.), with inter-rater comparisons demonstrating a high degree of agreement (intraclass correlation coefficient = 0.91; $p < .001$).

2.5. Statistical analyses

Statistical analyses were performed using R version 3.5.0 (The R Foundation, Vienna, Austria) (R Development Core Team, 2018) and SAS version 9.4 (The SAS institute, Cary, NC). Normality of data was assessed with the Shapiro-Wilk test, which determined the use of non-parametric methods for all data analyses. Descriptive statistics of clinical factors, including gestational age at birth, postmenstrual age at MRI scan, birth weight and clinical risk index scores (Rogers et al., 2016), as well as measured factors, including frontal-occipital horn ratio and dMRI measures in the LVP and FOHP, were obtained. Kruskal-Wallis one-way ANOVA was used to determine between groups differences. Wilcoxon signed rank test was used to perform family-wise comparisons, and all resulting p-values were corrected with Benjamini-Hochberg adjustment. Correlations between ventricular size and dMRI measures were examined using Spearman’s rank-order correlations because the patient groups correspond with disease severity (ordinal

Table 1.

Characteristics of 158 infants in a prospective study to assess the effects of IVH/PHH on dMRI measures of the lateral ventricular layer.

	Full term	Very preterm	High grade IVH	Post-hemorrhagic hydrocephalus
# of patients	56 (35.4%)	72 (45.6%)	17 (10.8%)	13 (8.2%)
Sex (# of Male/Female)	27 /29	30 /42	7/9	13/0
Birth gestational age (weeks)	39.0 ± 1.2	27.0 ± 1.7	25.0 ± 2.0	24.0 ± 2.1
Term age equivalent as scan (weeks)	39.0 ± 1.2	37.0 ± 1.5	38.0 ± 2.1	39.0 ± 1.1
Birth weight (g)	3229.50 ± 461.14	940 ± 257.67	735 ± 266.50	780 ± 216.27
Clinical risk index score	0.00 ± 0.00	1.00 ± 1.87	3.00 ± 1.69	3.00 ± 2.33
Frontal-occipital horn ratio	0.37 ± 0.02	0.41 ± 0.02	0.41 ± 0.04	0.50 ± 0.06

All measures within the respective groups are medians ± standard deviations where necessary.

ranking). To examine group differences in dMRI measures between the LVP and FOHP, a linear mixed effect model with a random patient intercept was fit to each measure. Specifications of the model included a main effect of region (LVP and FOHP), group (FT, VPT, HG-IVH and PHH) and region-by-group interactions with Bonferroni correction. Given the reported effect of age on dMRI measures (Yuan et al., 2013), postmenstrual age at scan was set as a covariate in the linear model. Where Mauchly’s test of sphericity was violated, Greenhouse-Geisser correction was used to adjust degrees of freedom for the averaged tests of significance. Significance level was determined using a p-value ≤ .05.

3. Results

3.1. Patient characteristics

Of the 158 infants (77 males and 81 females) included in the final study cohort, there were 56 FT, 72 VPT, 17 HG-IVH, and 13 PHH infants (Table 1; Supplementary Fig. 1). Median frontal-occipital horn ratios were higher in PHH (0.50 ± 0.06) > HG-IVH (0.41 ± 0.04) = VPT (0.41 ± 0.02) > FT (0.37 ± 0.02) (Table 1; Fig. 2). Of the 13 PHH infants, 12 had reservoirs and 2 had subgaleal shunts placed prior to VP shunt or ETV surgery. For permanent hydrocephalus treatment, 10 infants had VP shunts placed and 2 underwent ETV surgery. As expected, the median ventricular size of the ETV infants was larger (0.60 ± 0.01) than that of the VP shunt infants (0.49 ± 0.05) ($p = .008$). Nevertheless, in this limited cohort, there was no difference in dMRI measures between infants who underwent ETV versus VP shunt in both the LVP and FOHP regions. One infant underwent treatments for hydrocephalus with a reservoir but did not require permanent CSF diversion.

dMRI measures of the lateral ventricular perimeter and the frontal and occipital horn perimeters

In the LVP, family-wise comparisons with Benjamini-Hochberg correction revealed that PHH had consistently lower FA and higher MD and RD than FT and VPT infants ($p < .050$). While PHH FA was lower, and PHH RD was higher than that of HG-IVH ($p < .050$) in the LVP, the MD and AD values did not differ (Table 2; Fig. 3). In the FOHP, Benjamini-Hochberg corrected family-wise comparisons revealed PHH infants had lower FA and higher RD than FT and VPT infants in the FOHP ($p < .010$) (Table 2; Fig. 4). Similar to the LVP, PHH FA was lower than that of HG-IVH ($p < .001$) in the FOHP. Except for MD and RD in the LVP region, there were no differences in dMRI measures between the HG-IVH and VPT infants. Among the PHH group, there was no difference in dMRI measures between the ETV and VP shunt treated infants ($p > .050$) in both the LVP and FOHP regions. While the magnitude of PHH AD was consistently less than AD measures in the other groups, in both the LVP and FOHP pairwise comparisons were not significant ($p > .050$) (Tables 2; Figs. 3 and 4). Comparison of LVP/FOHP dMRI measures to those of adjacent posterior limb of internal capsule (PLIC) and optic radiations (OPRA) revealed tract-specific associations between dMRI measures. Among the HG-IVH infants, dMRI metrics in both the LVP and FOHP were associated with OPRA microstructure, but no associations were found with the PLIC. In contrast, few associations were found for the PHH group.

Table 2.
FA, MD, and RD among 158 full- and pre-term infants with/or without IVH/PHH.

	Median dMRI measures				Sig.	Groupwise Comparisons					
	FT	VPT	HG-IVH	PHH		FT: VPT	FT: HG-IVH	FT: PHH	VPT: HG-IVH	VPT: PHH	HG-IVH: PHH
Lateral ventricular perimeter											
FA	0.27 ± 0.05	0.23 ± 0.04	0.21 ± 0.04	0.16 ± 0.05	< 0.001*	< 0.001*	< 0.001*	< 0.001*	0.100	< 0.001*	0.004*
MD (μm ² /s)	1.46 ± 0.09	1.47 ± 0.08	1.55 ± 0.11	1.58 ± 0.15	< 0.001*	1.000	0.011*	0.027*	0.008*	0.034*	1.000
AD (μm ² /s)	1.88 ± 0.12	1.85 ± 0.15	1.93 ± 0.18	1.82 ± 0.25	0.031*	0.299	1.000	1.000	0.055	1.000	0.869
RD (μm ² /s)	1.24 ± 0.15	1.29 ± 0.12	1.38 ± 0.10	1.48 ± 0.15	< 0.001*	0.057	0.003*	< 0.001*	0.014*	< 0.001*	0.048*
Frontal occipital horn perimeter											
FA	0.29 ± 0.07	0.22 ± 0.06	0.20 ± 0.05	0.13 ± 0.04	< 0.001*	< 0.001*	< 0.001*	< 0.001*	0.349	< 0.001*	< 0.001*
MD (μm ² /s)	1.59 ± 0.11	1.66 ± 0.19	1.73 ± 0.14	1.77 ± 0.24	< 0.001*	0.022*	0.003*	0.102	0.213	0.700	1.000
AD (μm ² /s)	2.13 ± 0.14	2.09 ± 0.27	2.11 ± 0.21	1.94 ± 0.32	0.173	1.000	1.000	0.281	1.000	1.000	0.567
RD (μm ² /s)	1.33 ± 0.17	1.45 ± 0.18	1.56 ± 0.15	1.66 ± 0.24	< 0.001*	0.002*	< 0.001*	0.007*	0.118	0.007*	0.869

All measures within the respective groups are medians ± standard deviations where necessary; One-way ANOVA was performed with Kruskal-Wallis test (Sig.). All groupwise comparisons performed by Wilcoxon signed rank family-wise comparisons. All p-values are Benjamini-Hochberg corrected with alpha level set at $p < 0.050$ (*). FA = fractional anisotropy; MD = mean diffusivity; AD = axial diffusivity; RD = Radial diffusivity; PHH = post hemorrhagic hydrocephalus; HG-IVH = high grade intraventricular hemorrhage; VPT = very preterm; FT = full term.

3.2. Regional differences in dMRI measures

A linear mixed effects model, adjusted for term equivalent age at scan, revealed regional FA and RD differences between the FOHP and LVP [F (3,153) = (FA (19.46), MD (0.98), AD (1.88), RD (3.16); $p < .001$]. In the FT infants, FA, MD, AD and RD measures in the FOHP were higher than the LVP, which reflects baseline differences between the two regions among healthy infants in this cohort (Table 3; Fig. 5). However, in the PHH group, while MD, RD and AD measures in the FOHP were higher than the LVP, FOHP FA was less than the LVP, directly opposite to the observed findings in the healthy infants (Table 3; Fig. 5). Nevertheless, directionality of the principal eigenvectors in both LVP and FOHP generally did not differ between groups (Fig. 6).

3.3. Correlations between ventricular size and dMRI measures

Spearman's rho revealed that frontal-occipital horn ratio correlated with dMRI measures in the LVP. Ventricular size had negative correlation with FA ($r_s = -0.41$, $p < .001$), with anticipated positive correlations with MD ($r_s = 0.26$, $p = .005$) and RD ($r_s = 0.36$, $p < .001$) in the

LVP (Fig. 7). Relatively stronger relationships were found in the FOHP in that ventricular size was negatively correlated with FA ($r_s = -0.47$, $p < .001$) and positively correlated with MD ($r_s = 0.35$, $p < .001$) and RD ($r_s = 0.42$, $p < .001$) (Fig. 8). AD measures did not correlate with ventricular size in either the LVP or FOHP segmentation analyses ($r_s = -0.05$, $p = 1.000$).

4. Discussion

4.1. Summary of findings

This study utilized a large prospective cohort of preterm infants with and without HG-IVH/PHH and healthy, full-term controls to evaluate dMRI measures in the LVP and FOHP regions, neural stem cell rich areas important for neurodevelopment, brain-CSF homeostasis and immune response that function as a protective barrier to shield periventricular white matter from injurious CSF toxins (Alvarez and Teale, 2007; Mishra and Teale, 2012). To accomplish this, we developed a new image processing technique designed specifically to isolate the LVP and FOHP. The key findings were that PHH was associated with

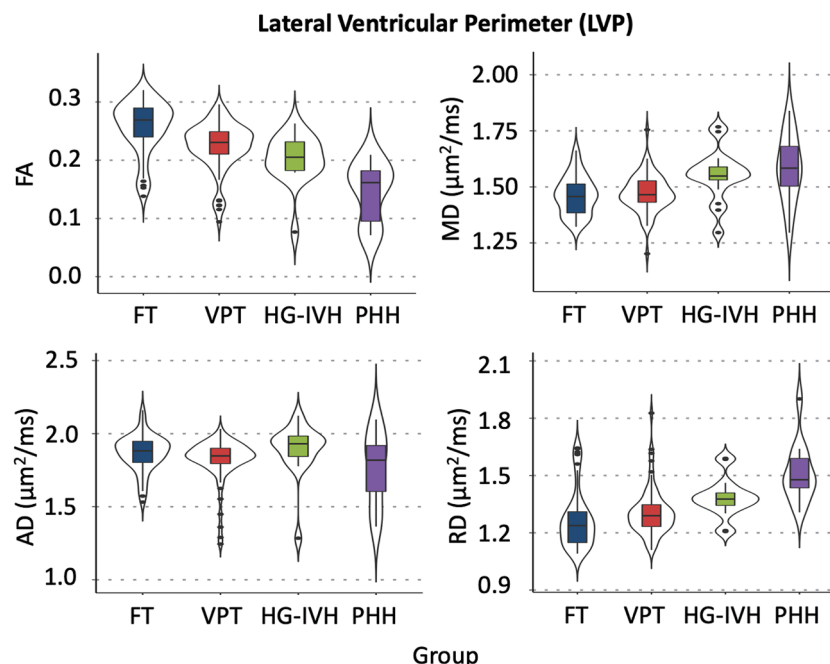


Fig. 3. dMRI measures of the lateral ventricular perimeter (LVP) demonstrating increasing severity of brain injury corresponds with decreasing fractional anisotropy (FA) and increasing mean (MD) and radial (RD) diffusivities. No significant changes were observed in axial diffusivity (AD) measures between groups.

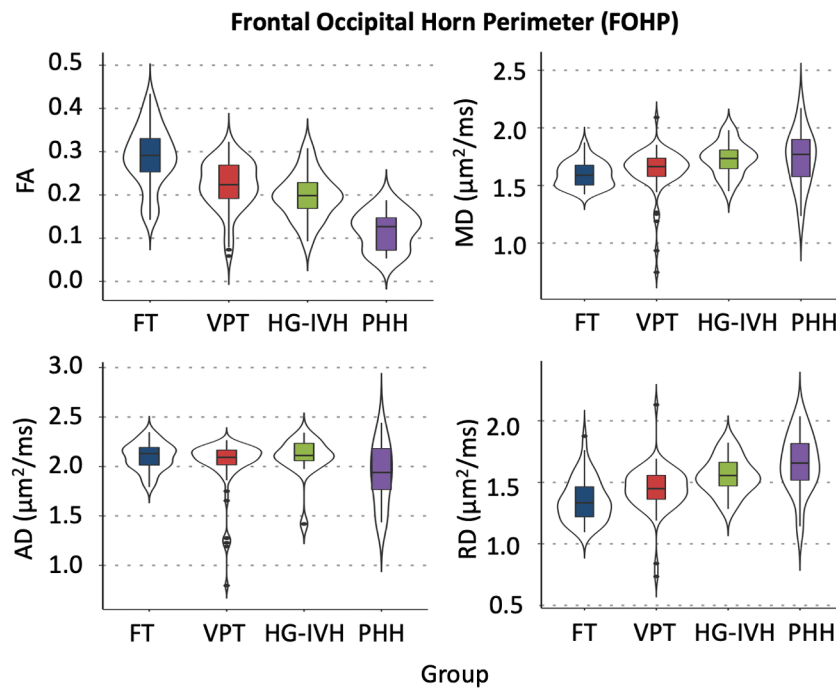


Fig. 4. dMRI measures of the frontal occipital horn perimeter (FOHP) demonstrating increasing severity of brain injury corresponds with decreasing fractional anisotropy (FA) and increasing mean (MD) and radial (RD) diffusivities. No significant differences were observed in axial diffusivity (AD) measures between groups.

aberrant measures of FA, MD and RD in these regions, indicative of disruptions in LVP and FOHP microstructure. The pattern of impaired RD but not AD may be associated with disruption of myelination or axonal membranes rather than axonal loss (Maxwell, 1996; Song et al., 2005; Sun et al., 2012). Among brain-injured infants, PHH infants demonstrated the greatest degree of abnormality, given their lower FA and higher MD and RD values when compared with the HG-IVH group. Except for MD and RD in the LVP region, there were no differences between HG-IVH and VPT infants, which suggests that while preterm birth has detrimental effects on dMRI measures, it does not solely account for the dMRI aberrations seen in the PHH group. In addition, markers of injury in the FOHP were of greater magnitude than in the LVP in the PHH group, indicating greater vulnerability to the effects of

injury in this region. Ventricular size correlated negatively with FA and positively with MD and RD in both the LVP and FOHP segmentations, suggesting increasing ventricular size was associated with more severe dMRI-measured LVP/FOHP injury.

4.2. Challenges and alternative strategies for delineating the LVP for dMRI analyses

The LVP, which has been histologically characterized as a critical region in IVH/PHH pathophysiology (Castaneyra-Ruiz et al., 2018; Jimenez et al., 2014; Jimenez et al., 2009; McAllister et al., 2017), is challenging to study with dMRI because of partial volume effects that may occur when adjacent or surrounding structures are included in the

Table 3. Region-specific dMRI measures in 158 infants examining the differences between-groups at the LVP and FOHP.

	Lateral ventricular perimeter		Frontal occipital horn perimeter			Mean difference (LVP-FOHP)	
	Estimate	Lower	Upper	Estimate	Lower		Upper
Fractional anisotropy							
FT	0.26	0.24	0.27	0.29	0.27	0.30	-0.03
VPT	0.22	0.21	0.24	0.22	0.21	0.23	0.00
HG-IVH	0.20	0.18	0.23	0.20	0.17	0.23	0.00
PHH	0.15	0.12	0.18	0.12	0.09	0.15	0.03
Mean diffusivity ($\mu\text{m}^2/\text{s}$)							
FT	1.46	1.42	1.50	1.60	1.56	1.63	-0.13
VPT	1.47	1.44	1.51	1.63	1.60	1.67	-0.16
HG-IVH	1.55	1.49	1.62	1.73	1.66	1.80	-0.17
PHH	1.58	1.51	1.66	1.73	1.65	1.81	-0.15
Axial diffusivity ($\mu\text{m}^2/\text{s}$)							
FT	1.88	1.82	1.93	2.11	2.05	2.16	-0.23
VPT	1.82	1.77	1.86	2.02	1.97	2.07	-0.20
HG-IVH	1.90	1.80	2.00	2.10	2.00	2.20	-0.20
PHH	1.77	1.66	1.88	1.92	1.81	2.03	-0.15
Radial diffusivity ($\mu\text{m}^2/\text{s}$)							
FT	1.26	1.22	1.31	1.35	1.31	1.39	-0.09
VPT	1.31	1.27	1.35	1.45	1.41	1.49	-0.14
HG-IVH	1.38	1.30	1.46	1.54	1.46	1.62	-0.16
PHH	1.51	1.42	1.60	1.65	1.56	1.74	-0.14

Summary of least square means from a linear mixed effects model, with patient age at which dMRI was obtained set as a covariate. PHH = post hemorrhagic hydrocephalus; HG-IVH = high grade intraventricular hemorrhage; VPT = very preterm; FT = full term. Lower and upper values are confident intervals.

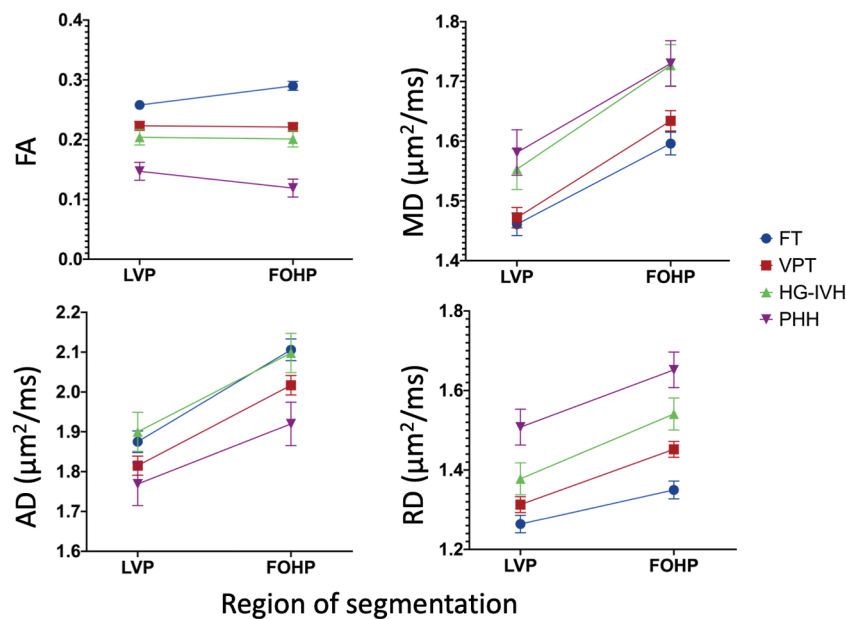


Fig. 5. Effects of region of segmentation on dMRI measures between groups demonstrating the FOHP in PHH had higher MD, AD and RD as well as lower FA measures than the LVP, an indication the FOHP is more disrupted than the LVP. Error bars are standard error means.

segmentation. This is because, in addition to being in close proximity to ventricular CSF and other tissues of varying signal intensities, the thickness of the LVP is only a few cell layers. Indeed, the ependymal layer is a single layer of epithelial cells (~5 μm thickness), and the ventricular and subventricular zones comprise a mix of radial glial and neuroblast cells (Jimenez et al., 2014; Kriegstein and Alvarez-Buylla, 2009), which makes it technically challenging to segment a homogeneous ROI for the LVP. In this study, the dMRI spatial resolution was $1.2 \times 1.2 \times 1.2 \text{ mm}^3$, and we evaluated the innermost layer of the LVP and its adjoining periventricular white matter. This voxel size is larger than the subventricular zone. As a result, the ROIs likely contain a mixture of subventricular zone and subjacent white matter. These ROIs had nonzero diffusion anisotropy, and evaluation of eigenvector maps (Fig. 6) showed fiber orientation parallel to the walls of the lateral ventricles, consistent with the orientation of white matter in these areas. In contrast, the subventricular zone would be expected to have isotropic diffusion or a primary orientation of maximum water displacements orthogonal to the walls of the lateral ventricles. Thus, the measured diffusion parameters likely reflect those of white matter, and injury to the subventricular zone is inferred through evidence of injury

to the adjacent white matter. Further, the ROIs were generated with an automated algorithm, which helped eliminate manual and inter-/intra-rater related errors. In addition, the ROIs were averaged from three contiguous axial slices to increase signal to noise and reduce through-plane partial volume averaging effects.

4.3. Clinical and research implications of LVP injury in IVH/PHH

Many of the debilitating symptoms of IVH/PHH have been attributed to periventricular white matter injury (Allin et al., 2011; Cherian et al., 2004; Shooman et al., 2009; Tsimis et al., 2016). As such, the anatomical, physiological and molecular relationships between the LVP and periventricular white matter have several critical research and clinical implications. First, IVH/PHH in preterm infants typically occurs during a critical developmental period of ventricular/subventricular zone differentiation, interfering with neural stem cell maturation and ependymal CSF-brain barrier formation. Impairment in ependymogenesis leads to denuded regions that expose periventricular white matter to injury from CSF contents, ciliopathy that impairs CSF circulation, and overall dysregulation of cerebral homeostasis, immunologic

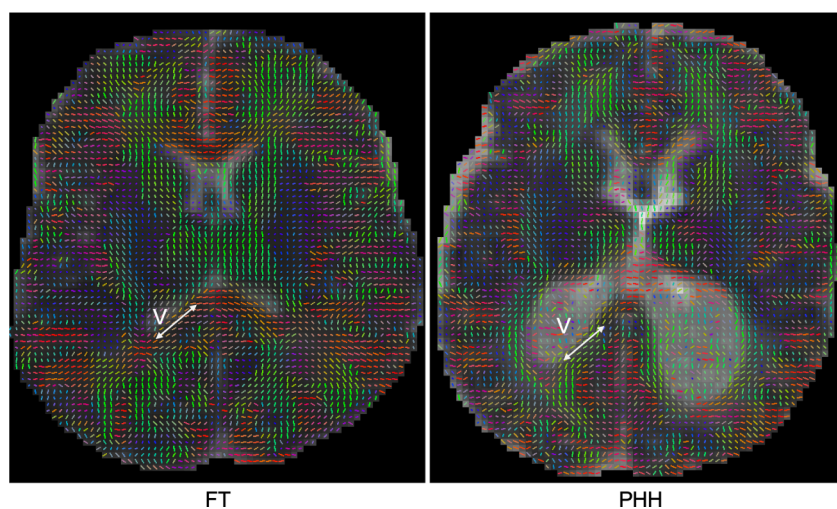


Fig. 6. Representative principal eigenvector maps of a healthy full-term (FT) and post hemorrhagic hydrocephalus (PHH) infant, demonstrating the orientation of the direction of maximum water displacements (arrows) along the perimeter of the ventricles (v) was generally preserved between groups in spite of the reduced anisotropy in the PHH group.

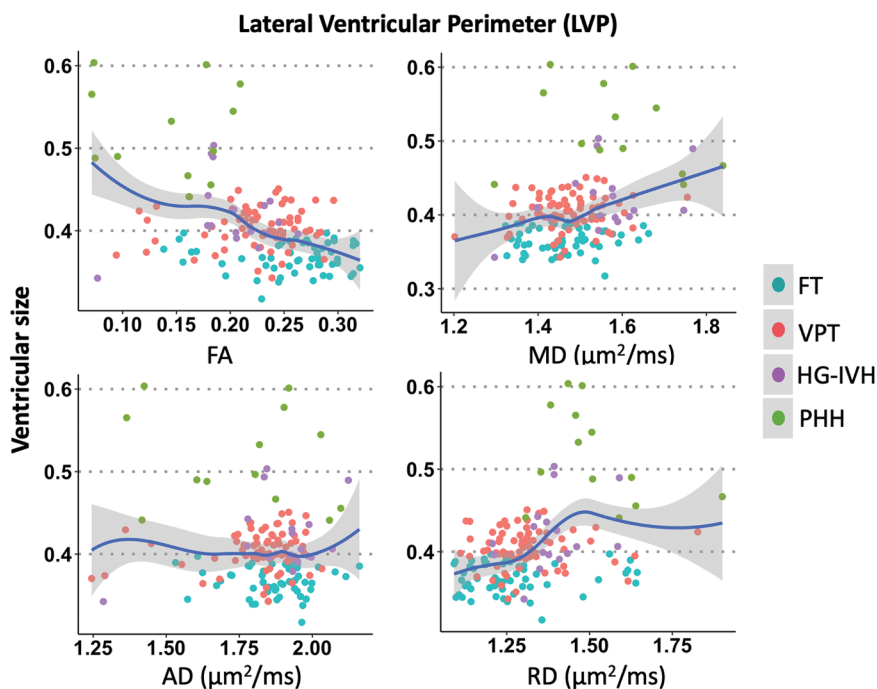


Fig. 7. dMRI-ventricular size correlations in the lateral ventricular perimeter (LVP) demonstrating larger ventricular size was associated with higher MD and RD and lower FA, suggesting ventricular enlargement is associated with dMRI-measured LVP disruption.

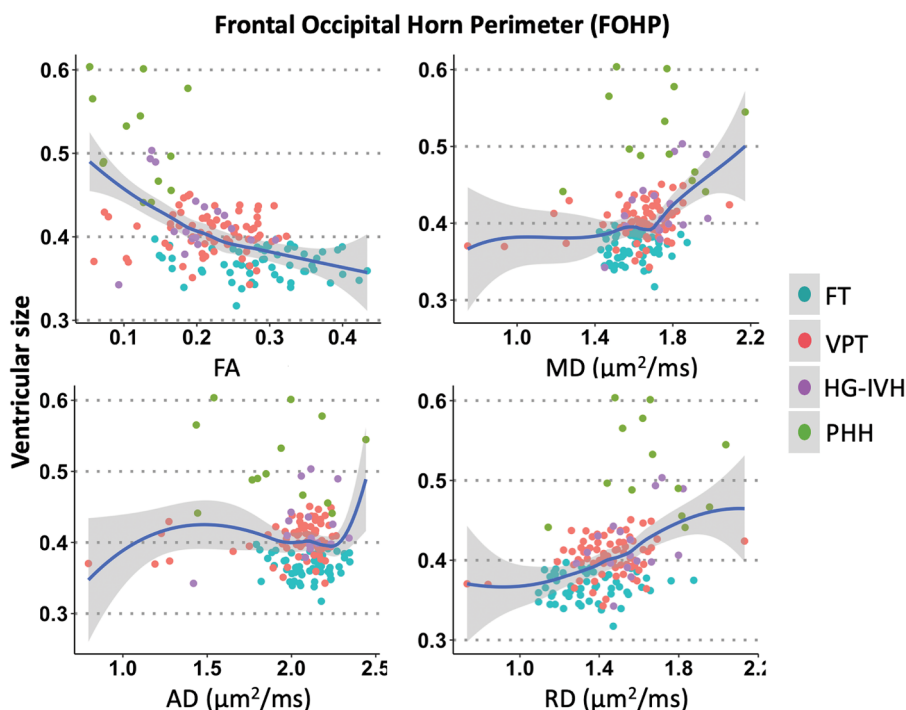


Fig. 8. dMRI-ventricular size correlations in the frontal occipital horn perimeter (FOHP) demonstrating larger ventricular size was associated with higher MD and RD and lower FA, suggesting ventricular enlargement is associated with dMRI-measured FOHP disruption.

response to injury and other normal cellular processes (Alvarez and Teale, 2007; Mishra and Teale, 2012). In addition, the irritation effects of blood, ferritin and reactive oxidative species likely propagates injurious mechanisms of neuroinflammation, hypoxia and ischemia (Del Bigio et al., 1994; McAllister et al., 2017) that further compromises the LVP barrier and damages periventricular white matter (Del Bigio, 1995; Di Curzio, 2018; Jimenez et al., 2014). Thus, examining LVP/FOHP tissue integrity with dMRI in IVH patients may help focus future research on strategies that enhance LVP barrier properties

in preterm infants to avert periventricular white matter injury and its neurological sequelae. Second, in PHH, the ventricular dilatation exerts mechanical pressure on both the LVP and periventricular white matter (Del Bigio, 2010; McAllister and Chovan, 1998), which may exacerbate ependymal denudation and axonal dysfunction due to direct axonal stretch and/or compression. Further, from a PHH treatment standpoint, CSF diversion surgery is typically performed to relieve the mechanical pressure to prevent further damage and permit recovery (Buckley et al., 2012; Mangano et al., 2016; Scheel et al., 2012). Therefore, utilizing

dMRI metrics to assess the relationships between ventricular size and LVP/FOHP integrity in IVH patients with or without PHH may help define the compounding effect of PHH on periventricular white matter on top of IVH, and the role of therapeutic ventricular decompression.

4.4. Cellular basis of dMRI-measured LVP injury in IVH/PHH

During typical white matter development, periventricular white matter FA increases, while MD, RD and AD decrease in a time-dependent fashion (Hüppi et al., 1998; Smyser et al., 2016). Our finding of lower FA and higher MD and RD in VPT than FT infants is consistent with previous studies that have shown that preterm birth is associated with dMRI-measured tissue abnormalities (Thompson et al., 2011; Thompson et al., 2014; Wu et al., 2017) and poor neurological outcomes, which have been attributed to disrupted neuronal proliferation, migration and synaptogenesis (Bockhorst et al., 2008). In HG-IVH and PHH the premature brain's sensitivity to perturbations in normal cellular processes by hemorrhage and hydrocephalus contributes significantly to their poorer neurological outcomes when compared to non-IVH preterm infants and healthy full term controls (Allin et al., 2011; Khwaja and Volpe, 2008; Tsimis et al., 2016). Our finding of more prominent abnormalities in FA, MD and RD in HG-IVH and PHH infants recapitulates the patterns of IVH/PHH-associated tissue injury that have been previously reported by dMRI studies of large bundle periventricular white matter tracts such as the corpus callosum and internal capsule (Akbari et al., 2015; Drobyshevsky et al., 2007; Lean et al., 2019; Mangano et al., 2016; Thompson et al., 2012). To propose a molecular mechanism for LVP injury in the setting of IVH, Castaneyra-Ruiz et al. utilized cell cultures of ventricular zone cells from the LVP to demonstrate ventricular zone disruption occurred as a result of cleavage of adherens junctions proteins (Castaneyra-Ruiz et al., 2018), thereby exposing the periventricular white matter to severe inflammation and gliosis (Castaneyra-Ruiz et al., 2018; McAllister et al., 2017). Several other histopathological studies have shown that IVH is associated with LVP tissue damage which is characterized by ependymal denudation, heterotopia and rosette formation, radial glial cell disorganization, and astrocytic proliferation in the ventricular and subventricular zones (Dominguez-Pinos et al., 2005; Jimenez et al., 2009; McAllister et al., 2017). Ultimately, the poor neurological outcomes observed in HG-IVH/PHH infants are not only due to white matter injury, but are mediated by a complex interaction of pathophysiological mechanisms such as iron-mediated oxidative damage (Cherian et al., 2004), hypoxic-ischemic injury (Salmaso et al., 2014), cytokine-chemokine mediated injury (Castaneyra-Ruiz et al., 2018; McAllister et al., 2017) and deleterious complement activation (Ryckman et al., 2011) that culminate in grey and white matter brain injury.

4.5. IVH/PHH-associated injury in the LVP/FOHP may impair myelination

Diffusion anisotropy data in white matter are typically interpreted in terms of changes to myelin, with an increase in RD thought to represent injury to myelin with relative sparing of axons. In the present context, this interpretation is complicated by the fact that most of periventricular white matter is not myelinated at term equivalent (Sarnat, 1992). While white matter tracts associated with primary motor and sensory areas, particularly corticospinal tracts and optic radiations, are myelinated at term equivalent and do show greater values for diffusion anisotropy than unmyelinated areas (Smyser et al., 2016), the majority of periventricular white matter is unmyelinated at this stage of development (Sarnat, 1992). Thus, for this study, the relative increase in RD compared with AD suggests greater spacing of axons, possibly related to transependymal migration of CSF, and/or an increase in axonal membrane permeability, perhaps related to stretching and injury (Maxwell, 1996; Song et al., 2005; Sun et al., 2012). The influence of these unmyelinated axons on the diffusion

measurement is supported by the finding that the orientation of the direction of maximum water displacements (which indicates the orientation of white matter fiber tracts) was generally preserved in spite of the reduced anisotropy, indicating that the axons were still present. Nevertheless, disruption of the LVP may be associated with subsequent abnormalities of myelination through injury to oligodendrocyte progenitor cells that are present in this region at term equivalent. Indeed studies of the corpus callosum of older hydrocephalic children after myelination (Akbari et al., 2015; Yuan et al., 2013) show MD changes driven by changes RD rather than by AD, indicating myelin disruption. Other studies have identified morphological defects in oligodendrocytes, which occur as a result of hemorrhage and other multifactorial mechanisms, including neuroinflammation and ischemia-induced excitotoxicity (Aisengart et al., 2011; Ayannuga and Naicker, 2017; Castejon et al., 2001; Di Curzio et al., 2013; Goto et al., 2008; Miller and McAllister, 2007). In addition, PHH likely compounds oligodendrocyte disruption and periventricular white matter dysmyelination through its compressive effects on oligodendrocyte progenitor cells in the LVP (Aisengart et al., 2011; Ayannuga and Naicker, 2017; Castejon et al., 2001).

4.6. FOHP sustains a greater magnitude of dMRI-measured injury than the LVP

Across the LVP, there are regional differences in the cytoarchitecture of the ventricular zone and organization of neural stem cells within the subjacent subventricular zones (Jimenez et al., 2014; McAllister et al., 2017). While radial glial cells are sequentially replaced by ependymal cells along the LVP during fetal development, the lateral wall of the frontal horn is the only region that retains these stem cells into infancy (Coletti et al.), which may contribute to adverse neurodevelopmental outcomes when those regions are damaged by IVH/PHH. Indeed, in our cohort, the FOHP demonstrated more prominent evidence of injury than the LVP. These findings are consistent with the more prominent patterns of FOHP than LVP injury seen on conventional MRI scans of hydrocephalus patients, which is characterized by periventricular hyperintensities on T₂W imaging that represent severe tissue disruption (Khwaja and Volpe, 2008; McMenamin et al., 1984), susceptibility weighted findings of petechial hemorrhages that are caused by elevated medullary vein pressures (Childs et al., 2001; Niwa et al., 2011; Perlman, 1998) and restricted diffusion suggestive of tissue ischemia (Bassan et al., 2006). There is also a disproportionate distribution of stress and strain on the stem cell rich FOHP in patients with hydrocephalus (Kim et al., 2015; Nagashima et al., 1987; Pena et al., 1999). For example, relative to the LVP, the FOHP region is subjected to higher stress and strain in the setting of hydrocephalus because of its concave geometry and acute anterolateral angles, which in turn expands the extracellular spaces in the FOHP and facilitates water extravasation and tissue edema (Kim et al., 2015; Nagashima et al., 1987; Pena et al., 1999). It is important to note however, that in this study, all PHH infants had undergone intervention for hydrocephalus, and their intracranial pressure was expected to have normalized at the time of dMRI acquisition. Nevertheless, we suspect the dMRI disruptions seen in the PHH group may reflect complex pathology from the initial IVH, injury from raised intracranial pressure sustained prior to their shunt/ETV treatment, and the subsequent associated secondary injury.

4.7. Ventricular size positively correlates with magnitude LVP injury

Collectively, the tensile and compressive forces of enlarged ventricles (including in PHH) on the FOHP and the remainder of the LVP leads to impairment of arterial blood flow and venous stasis, which may cause axonal disruption and dysmyelination that sets off a cascade of ischemia-induced white matter injury (Ayannuga and Naicker, 2017; Hagberg et al., 2002; Soul et al., 2004). These findings beg the question

whether ventricular size can be used as a surrogate marker for disease severity in PHH patients. In our cohort, ventricular size correlated negatively with FA and positively with MD and RD, suggesting that expanded ventricular size likely has a negative effect on dMRI-measured LVP/FOHP tissue integrity. However, subgroup analysis of the PHH group alone did not yield meaningful correlations. Our findings reflect the ongoing debate on ventricular size-dMRI correlations, as variable results have been reported in the literature (Akbari et al., 2015; Cauley and Cataltepe, 2014; Kulkarni et al., 2015). While our study suggests increasing ventricular size negatively affects LVP/FOHP integrity, a larger population of PHH patients, including studies before and after treatment of hydrocephalus and correlative histological analyses, are required to better understand the clinical implications.

4.8. Limitations

A primary limitation of this study is the small sample size in the PHH and, to a lesser extent, HG-IVH cohorts which may have limited our ability to observe subtle differences in periventricular dMRI parameters, especially in the FOHP. As 6 PHH infants with extensive injury were unable to be included in the MRI analysis, results may not generalize to other higher-risk cohorts of PHH infants, including those demonstrating the most severe forms of injury. Additionally, all 13 PHH patients included in current analyses were male, which may have introduced a sex bias in the PHH group, although there is a male preponderance in IVH reported in the literature (Cuestas et al., 2009; Tioseco et al., 2006). Another limitation is that our study contained only term-equivalent scans with a cross-sectional design. A longitudinal study including multiple scans at predetermined time-points for each subject would allow more detailed evaluation of relationships between dMRI parameters, frontal-occipital horn ratio, and neurobehavioral correlates over time. In addition, future studies should investigate prospective associations between dMRI measures in the LVP and FOHP with subsequent neurodevelopmental outcomes to elucidate the neurological mechanisms underlying impairment in high-risk VPT infants, as well as to potentially identify VPT infants in need of early referral to intervention services and longer-term follow-up care.

5. Conclusion

dMRI demonstrates that HG-IVH and PHH are associated with microstructural injury/disruption of LVP/FOHP. The patterns of LVP/FOHP injury in this cohort of infants were attributable to axonal spacing likely secondary to transependymal CSF migration, and/or increased axonal membrane permeability, perhaps associated with stretching and injury. Infants with PHH demonstrated the most aberrant dMRI measures, more profoundly in the FOHP, which may be attributed to compounding mechanical injury caused by pressures exerted on the LVP/FOHP regions by the expanded ventricles. Given the LVP/FOHP's critical role in neurodevelopment and cerebral function, the observed impairments in tissue integrity may contribute to the debilitating sequelae of IVH/PHH. Future studies are required to assess histological correlates of our findings, and additional work is needed to confirm these observations in longitudinal studies which characterize changes in these relationships over time and their relationships with neurodevelopment outcomes. Given the role of the LVP/FOHP in IVH/PHH disease pathophysiology and dMRI's capability to detect LVP/FOHP tissue integrity, as well as its correlation with ventricular size, the LVP/FOHP may provide useful biomarkers of IVH/PHH for future clinical studies directed at improving the clinical management of these conditions.

Acknowledgements

We thank Dr. Joseph N. Paulson (Genentech, San Francisco, CA, USA) for his help with the statistical analyses; Ms. Karen Lukas, Mr.

Anthony Barton, and Ms. Jessica Perkins for study coordination; Ms. Tara Smyser and Ms. Jeanette Kenley for their help with many aspects of data acquisition and analyses; IDDRC at Washington University for assistance with data collection; and the children and their families for participating in the study. We appreciate the support of our funding agencies including the National Institutes of Health, Child Neurology Foundation, Cerebral Palsy International Research Foundation, Dana Foundation, March of Dimes Prematurity Research Center at Washington University, Doris Duke Charitable Foundation, Eunice Kennedy Shriver National Institute of Child Health & Human Development of the National Institutes of Health. The funding sources had no involvement in study design, data analysis, writing the report, or the decision to submit the article for publication.

Supplementary materials

Supplementary material associated with this article can be found, in the online version, at [doi:10.1016/j.nicl.2019.102031](https://doi.org/10.1016/j.nicl.2019.102031).

References

- Adams-Chapman, I., Hansen, N.I., Stoll, B.J., Higgins, R., Network, N.R., 2008. Neurodevelopmental outcome of extremely low birth weight infants with post-hemorrhagic hydrocephalus requiring shunt insertion. *Pediatrics* 121 e1167-1177.
- Aisengart, B., Kajiwara, J.K., Verissimo Meira, K., da Silva Lopes, L., 2011. Morphometric analysis of the optic nerve in experimental hydrocephalus-induced rats. *Pediatr. Neurosurg.* 47, 342-348.
- Akbari, S.H., Limbrick Jr., D.D., McKinstry, R.C., Altaye, M., Ragan, D.K., Yuan, W., et al., 2015. Periventricular hyperintensity in children with hydrocephalus. *Pediatr. Radiol.* 45, 1189-1197.
- Allin, M.P., Kontis, D., Walshe, M., Wyatt, J., Barker, G.J., Kanaan, R.A., et al., 2011. White matter and cognition in adults who were born preterm. *PLoS ONE* 6, e24525.
- Alvarez, J.I., Teale, J.M., 2007. Differential changes in junctional complex proteins suggest the ependymal lining as the main source of leukocyte infiltration into ventricles in murine neurocysticercosis. *J. Neuroimmunol.* 187, 102-113.
- Ancel, P.Y., Livinec, F., Larroque, B., Marret, S., Arnaud, C., Pierrat, V., et al., 2006. Cerebral palsy among very preterm children in relation to gestational age and neonatal ultrasound abnormalities: the EPIPAGE cohort study. *Pediatrics* 117, 828-835.
- Assaf, Y., Ben-Sira, L., Constantini, S., Chang, L.C., Beni-Adani, L., 2006. Diffusion tensor imaging in hydrocephalus: initial experience. *AJNR Am. J. Neuroradiol.* 27, 1717-1724.
- Ayannuga, O.A., Naicker, T., 2017. Cortical oligodendrocytes in kaolin-induced hydrocephalus in wistar rat: impact of degree and duration of ventriculomegaly. *Ann. Neurosci.* 24, 164-172.
- Bassan, H., Feldman, H.A., Limperopoulos, C., Benson, C.B., Ringer, S.A., Veracruz, E., et al., 2006. Periventricular hemorrhagic infarction: risk factors and neonatal outcome. *Pediatr. Neurol.* 35, 85-92.
- Bockhorst, K.H., Narayana, P.A., Liu, R., Ahobila-Vijjula, P., Ramu, J., Kamel, M., et al., 2008. Early postnatal development of rat brain: in vivo diffusion tensor imaging. *J. Neurosci. Res.* 86, 1520-1528.
- Brat, D.J., 2010. 2 - normal brain histopathology. In: Perry, A, Brat, DJ (Eds.), *Practical Surgical Neuropathology*. Churchill Livingstone, New York, pp. 15-33.
- Buckley, R.T., Yuan, W., Mangano, F.T., Phillips, J.M., Powell, S., McKinstry, R.C., et al., 2012. Longitudinal comparison of diffusion tensor imaging parameters and neuropsychological measures following endoscopic third ventriculostomy for hydrocephalus. *J. Neurosurg. Pediatr.* 9, 630-635.
- Bystron, I., Blakemore, C., Rakic, P., 2008. Development of the human cerebral cortex: boulder committee revisited. *Nat. Rev. Neurosci.* 9, 110-122.
- Castaneya-Ruiz, L., Morales, D.M., McAllister, J.P., Brody, S.L., Isaacs, A.M., Strahle, J.M., et al., 2018. Blood exposure causes ventricular zone disruption and glial activation in vitro. *J. Neuropathol. Exp. Neurol.* 77, 803-813.
- Castejon, O.J., Castejon, H.V., Castellano, A., 2001. Oligodendroglial cell damage and demyelination in infant hydrocephalus. An electron microscopic study. *J. Submicrosc. Cytol. Pathol.* 33, 33-40.
- Cauley, K.A., Cataltepe, O., 2014. Axial diffusivity of the corona radiata correlated with ventricular size in adult hydrocephalus. *AJR Am. J. Roentgenol.* 203, 170-179.
- Cherian, S., Whitelaw, A., Thoresen, M., Love, S., 2004. The pathogenesis of neonatal post-hemorrhagic hydrocephalus. *Brain Pathol.* 14, 305-311.
- Childs, A.M., Ramenghi, L.A., Cornette, L., Tanner, S.F., Arthur, R.J., Martinez, D., et al., 2001. Cerebral maturation in premature infants: quantitative assessment using MR imaging. *Am. J. Neuroradiol.* 22, 1577-1582.
- Coletti A.M., Singh D., Kumar S., Shafin T.N., Briody P.J., Babbitt B.F., et al.: Characterization of the ventricular-subventricular stem cell niche during human brain development. *Development* 145, 2018.
- Cuestas, E., Bas, J., Pautasso, J., 2009. Sex differences in intraventricular hemorrhage rates among very low birth weight newborns. *Gend. Med.* 6, 376-382.
- Del Bigio, M.R., 1995. The ependyma: a protective barrier between brain and cerebrospinal fluid. *Glia* 14, 1-13.
- Del Bigio, M.R., 2010. Neuropathology and structural changes in hydrocephalus. *Dev.*

- Disabil. Res. Rev. 16, 16–22.
- Del Bigio, M.R., da Silva, M.C., Drake, J.M., Tuor, U.I., 1994. Acute and chronic cerebral white matter damage in neonatal hydrocephalus. *Can. J. Neurol. Sci.* 21, 299–305.
- Di Curzio, D.L., 2018. Neuropathological changes in hydrocephalus—a comprehensive review. *Open J. Mod. Neurosurg.* 08, 1–29.
- Di Curzio, D.L., Buist, R.J., Del Bigio, M.R., 2013. Reduced subventricular zone proliferation and white matter damage in juvenile ferrets with kaolin-induced hydrocephalus. *Exp. Neurol.* 248, 112–128.
- Dominguez-Pinos, M.D., Paez, P., Jimenez, A.J., Weil, B., Arraez, M.A., Perez-Figures, J.M., et al., 2005. Ependymal denudation and alterations of the subventricular zone occur in human fetuses with a moderate communicating hydrocephalus. *J. Neuropathol. Exp. Neurol.* 64, 595–604.
- Drobyshevsky, A., Bregman, J., Storey, P., Meyer, J., Prasad, P.V., Derrick, M., et al., 2007. Serial diffusion tensor imaging detects white matter changes that correlate with motor outcome in premature infants. *Dev. Neurosci.* 29, 289–301.
- du Plessis, A.J., 2009. The role of systemic hemodynamic disturbances in prematurity-related brain injury. *J. Child Neurol.* 24, 1127–1140.
- Goto, J., Tezuka, T., Nakazawa, T., Sagara, H., Yamamoto, T., 2008. Loss of Fyn tyrosine kinase on the C57BL/6 genetic background causes hydrocephalus with defects in oligodendrocyte development. *Mol. Cell Neurosci.* 38, 203–212.
- Gotz, M., Huttner, W.B., 2005. The cell biology of neurogenesis. *Nat. Rev. Mol. Cell Biol.* 6, 777–788.
- Hagberg, H., Peebles, D., Mallard, C., 2002. Models of white matter injury: comparison of infectious, hypoxic-ischemic, and excitotoxic insults. *Ment. Retard. Dev. Disabil. Res. Rev.* 8, 30–38.
- Ho, M.-L., Rojas, R., Eisenberg, R.L., 2012. Cerebral edema. *Am. J. Roentgenol.* 199, W258–W273.
- Hüppi, P.S., Maier, S.E., Peled, S., Zientara, G.P., Barnes, P.D., Jolesz, F.A., et al., 1998. Microstructural development of human newborn cerebral white matter assessed in vivo by diffusion tensor magnetic resonance imaging. *Pediatr. Res.* 44, 584–590.
- Inder, T.E., Perlman, J.M., Volpe, J.J., et al., 2018. Chapter 24 - Preterm Intraventricular hemorrhage/posthemorrhagic hydrocephalus. In: Volpe, J.J., Inder, T.E., Darras, B.T., de Vries, L.S., du Plessis, A.J., Neil, J.J. (Eds.), *Volpe's Neurology of the Newborn* (Sixth Edition). Elsevier 637-698.e621.
- Jimenez, A.J., Dominguez-Pinos, M.D., Guerra, M.M., Fernandez-Llebrez, P., Perez-Figures, J.M., 2014. Structure and function of the ependymal barrier and diseases associated with ependyma disruption. *Tissue Barriers* 2, e28426.
- Jimenez, A.J., Garcia-Verdugo, J.M., Gonzalez, C.A., Batiz, L.F., Rodriguez-Perez, L.M., Paez, P., et al., 2009. Disruption of the neurogenic niche in the subventricular zone of postnatal hydrocephalic hyh mice. *J. Neuropathol. Exp. Neurol.* 68, 1006–1020.
- Kahle, K.T., Kulkarni, A.V., Limbrick Jr., D.D., Warf, B.C., 2016. Hydrocephalus in children. *Lancet* 387, 788–799.
- Khwaja, O., Volpe, J.J., 2008. Pathogenesis of cerebral white matter injury of prematurity. *Arch. Dis. Child Fetal Neonatal Ed.* 93 F153-161.
- Kim, H., Min, B.K., Park, D.H., Hawi, S., Kim, B.J., Czosnyka, Z., et al., 2015. Porohyperelastic anatomical models for hydrocephalus and idiopathic intracranial hypertension. *J. Neurosurg.* 122, 1330–1340.
- Klebermass-Schrehof, K., Czaba, C., Olschkar, M., Fuiko, R., Waldhoer, T., Rona, Z., et al., 2012. Impact of low-grade intraventricular hemorrhage on long-term neurodevelopmental outcome in preterm infants. *Childs Nerv. Syst.* 28, 2085–2092.
- Koschnitzky, J.E., Keep, R.F., Limbrick Jr., D.D., McAllister 2nd, J.P., Morris, J.A., Strahle, J., et al., 2018. Opportunities in posthemorrhagic hydrocephalus research: outcomes of the hydrocephalus association posthemorrhagic hydrocephalus workshop. *Fluids Barriers CNS* 15, 11.
- Kriegstein, A., Alvarez-Buylla, A., 2009. The glial nature of embryonic and adult neural stem cells. *Annu. Rev. Neurosci.* 32, 149–184.
- Kroenke, C.D., Bretthorst, G.L., Inder, T.E., Neil, J.J., 2006. Modeling water diffusion anisotropy within fixed newborn primate brain using Bayesian probability theory. *Magn. Reson. Med.* 55, 187–197.
- Kulkarni, A.V., Donnelly, R., Mabbott, D.J., Widjaja, E., 2015. Relationship between ventricular size, white matter injury, and neurocognition in children with stable, treated hydrocephalus. *J. Neurosurg.-Pediatr.* 16, 267–274.
- Lean, R.E., Han, R.H., Smyser, T.A., Kenley, J.K., Shimony, J.S., Rogers, C.E., et al., 2019. Altered neonatal white and gray matter microstructure is associated with neurodevelopmental impairments in very preterm infants with high-grade brain injury. *Pediatr. Res.*
- Liu, L., Oza, S., Hogan, D., Chu, Y., Perin, J., Zhu, J., et al., 2016. Global, regional, and national causes of under-5 mortality in 2000–15: an updated systematic analysis with implications for the sustainable development goals. *Lancet* 388, 3027–3035.
- Mangano, F.T., Altaye, M., McKinstry, R.C., Shimony, J.S., Powell, S.K., Phillips, J.M., et al., 2016. Diffusion tensor imaging study of pediatric patients with congenital hydrocephalus: 1-year postsurgical outcomes. *J. Neurosurg. Pediatr.* 18, 306–319.
- Mathur, A.M., Neil, J.J., McKinstry, R.C., Inder, T.E., 2008. Transport, monitoring, and successful brain MR imaging in unselected neonates. *Pediatr. Radiol.* 38, 260–264.
- Maxwell, W.L., 1996. Histopathological changes at central nodes of Ranvier after stretch-injury. *Microsc. Res. Tech.* 34, 522–535.
- McAllister 2nd, J.P., Chovan, P., 1998. Neonatal hydrocephalus. Mechanisms and consequences. *Neurosurg. Clin. N. Am.* 9, 73–93.
- McAllister 2nd, J.P., Williams, M.A., Walker, M.L., Kestle, J.R., Relkin, N.R., Anderson, A.M., et al., 2015. An update on research priorities in hydrocephalus: overview of the third national institutes of health-sponsored symposium "Opportunities for hydrocephalus research: pathways to better outcomes". *J. Neurosurg.* 123, 1427–1438.
- McAllister, J.P., Guerra, M.M., Ruiz, L.C., Jimenez, A.J., Dominguez-Pinos, D., Sival, D., et al., 2017. Ventricular zone disruption in human neonates with intraventricular hemorrhage. *J. Neuropathol. Exp. Neurol.* 76, 358–375.
- McMenamin, J.B., Shackelford, G.D., Volpe, J.J., 1984. Outcome of neonatal intraventricular hemorrhage with periventricular echodense lesions. *Ann. Neurol.* 15, 285–290.
- Miller, J.M., McAllister 2nd, J.P., 2007. Reduction of astrogliosis and microgliosis by cerebrospinal fluid shunting in experimental hydrocephalus. *Cerebrospinal Fluid Res.* 4, 5.
- Mishra, P.K., Teale, J.M., 2012. Transcriptome analysis of the ependymal barrier during murine neurocysticercosis. *J. Neuroinflammation.* 9, 141.
- Mukerji, A., Shah, V., Shah, P.S., 2015. Periventricular/Intraventricular hemorrhage and neurodevelopmental outcomes: a meta-analysis. *Pediatrics* 136, 1132–1143.
- Nagashima, T., Tamaki, N., Matsumoto, S., Horwitz, B., Seguchi, Y., 1987. Biomechanics of hydrocephalus: a new theoretical model. *Neurosurgery* 21, 898–904.
- Neil, J.J., Shiran, S.I., McKinstry, R.C., Schefft, G.L., Snyder, A.Z., Almlí, C.R., et al., 1998. Normal brain in human newborns: apparent diffusion coefficient and diffusion anisotropy measured by using diffusion tensor MR imaging. *Radiology* 209, 57–66.
- Niwa, T., de Vries, L.S., Benders, M.J.N.L., Takahara, T., Nikkels, P.G.J., Groenendaal, F., 2011. Punctate white matter lesions in infants: new insights using susceptibility-weighted imaging. *Neuroradiology* 53, 669–679.
- O'Hayon, B.B., Drake, J.M., Ossip, M.G., Tuli, S., Clarke, M., 1998. Frontal and occipital horn ratio: a linear estimate of ventricular size for multiple imaging modalities in pediatric hydrocephalus. *Pediatr. Neurosurg.* 29, 245–249.
- Papile, L.A., Burstein, J., Burstein, R., Koffler, H., 1978. Incidence and evolution of subependymal and intraventricular hemorrhage: a study of infants with birth weights less than 1,500 gm. *J. Pediatr.* 92, 529–534.
- Patra, K., Wilson-Costello, D., Taylor, H.G., Mercuri-Minich, N., Hack, M., 2006. Grades I–II intraventricular hemorrhage in extremely low birth weight infants: effects on neurodevelopment. *J. Pediatr.* 149, 169–173.
- Pena, A., Bolton, M.D., Whitehouse, H., Pickard, J.D., 1999. Effects of brain ventricular shape on periventricular biomechanics: a finite-element analysis. *Neurosurgery* 45, 107–116 discussion 116-108.
- Perlman, J.M., 1998. White matter injury in the preterm infant: an important determination of abnormal neurodevelopment outcome. *Early Hum. Dev.* 53, 99–120.
- Pierpaoli, C., Jezzard, P., Basser, P.J., Barnett, A., Di Chiro, G., 1996. Diffusion tensor MR imaging of the human brain. *Radiology* 201, 637–648.
- R Development Core Team, 2018. R: A language and Environment for Statistical Computing, in, Ed 3.5.0. R Foundation for Statistical Computing, Vienna, Australia.
- Robinson, S., 2012. Neonatal posthemorrhagic hydrocephalus from prematurity: pathophysiology and current treatment concepts. *J. Neurosurg. Pediatr.* 9, 242–258.
- Rogers, C.E., Smyser, T., Smyser, C.D., Shimony, J., Inder, T.E., Neil, J.J., 2016. Regional white matter development in very preterm infants: perinatal predictors and early developmental outcomes. *Pediatr. Res.* 79, 87–95.
- Ryckman, K.K., Dagle, J.M., Kelsey, K., Momany, A.M., Murray, J.C., 2011. Replication of genetic associations in the inflammation, complement, and coagulation pathways with intraventricular hemorrhage in lbw preterm neonates. *Pediatr. Res.* 70, 90.
- Salmaso, N., Jablonska, B., Scafidi, J., Vaccarino, F.M., Gallo, V., 2014. Neurobiology of premature brain injury. *Nat. Neurosci.* 17, 341–346.
- Sarnat, H.B., 1992. *Cerebral Dysgenesis: Embryology and Clinical Expression*. Oxford University Press, New York.
- Scheel, M., Diekhoff, T., Sprung, C., Hoffmann, K.T., 2012. Diffusion tensor imaging in hydrocephalus-findings before and after shunt surgery. *Acta Neurochir. (Wien)* 154, 1699–1706.
- Segev, Y., Metsker, U., Beni-Adani, L., Elran, C., Reider II, G., Constantini, S., 2001. Morphometric study of the midsagittal MR imaging plane in cases of hydrocephalus and atrophy and in normal brains. *AJNR Am. J. Neuroradiol.* 22, 1674–1679.
- Sherlock, R.L., Anderson, P.J., Doyle, L.W., Victorian Infant Collaborative Study, G., 2005. Neurodevelopmental sequelae of intraventricular haemorrhage at 8 years of age in a regional cohort of ELBW/very preterm infants. *Early Hum. Dev.* 81, 909–916.
- Shoeman, D., Portess, H., Sparrow, O., 2009. A review of the current treatment methods for posthaemorrhagic hydrocephalus of infants. *Cerebrospinal Fluid Res.* 6, 1.
- Smyser, T.A., Smyser, C.D., Rogers, C.E., Gillespie, S.K., Inder, T.E., Neil, J.J., 2016. Cortical gray and adjacent white matter demonstrate synchronous maturation in very preterm infants. *Cereb. Cortex* 26, 3370–3378.
- Song, S.K., Yoshino, J., Le, T.Q., Lin, S.J., Sun, S.W., Cross, A.H., et al., 2005. Demyelination increases radial diffusivity in corpus callosum of mouse brain. *Neuroimage* 26, 132–140.
- Soul, J.S., Eichenwald, E., Walter, G., Volpe, J.J., du Plessis, A.J., 2004. CSF removal in infantile posthemorrhagic hydrocephalus results in significant improvement in cerebral hemodynamics. *Pediatr. Res.* 55, 872–876.
- Stoll, B.J., Hansen, N.I., Bell, E.F., Walsh, M.C., Carlo, W.A., Shankaran, S., et al., 2015. Trends in care practices, morbidity, and mortality of extremely preterm neonates, 1993–2012. *JAMA* 314, 1039–1051.
- Sun, W., Fu, Y., Shi, Y., Cheng, J.X., Cao, P., Shi, R., 2012. Paranodal myelin damage after acute stretch in Guinea pig spinal cord. *J. Neurotrauma* 29, 611–619.
- Thompson, D.K., Inder, T.E., Faggian, N., Johnston, L., Warfield, S.K., Anderson, P.J., et al., 2011. Characterization of the corpus callosum in very preterm and full-term infants utilizing MRI. *Neuroimage* 55, 479–490.
- Thompson, D.K., Inder, T.E., Faggian, N., Warfield, S.K., Anderson, P.J., Doyle, L.W., et al., 2012. Corpus callosum alterations in very preterm infants: perinatal correlates and 2 year neurodevelopmental outcomes. *Neuroimage* 59, 3571–3581.
- Thompson, D.K., Thai, D., Kelly, C.E., Leemans, A., Tournier, J.D., Kean, M.J., et al., 2014. Alterations in the optic radiations of very preterm children-Perinatal predictors and relationships with visual outcomes. *Neuroimage Clin.* 4, 145–153.
- Tioseco, J.A., Aly, H., Essers, J., Patel, K., El-Mohandes, A.A., 2006. Male sex and intraventricular hemorrhage. *Pediatr. Crit. Care Med.* 7, 40–44.
- Tsimis, M.E., Johnson, C.T., Raghunathan, R.S., Northington, F.J., Burd, I., Graham, E.M., 2016. Risk factors for periventricular white matter injury in very low birthweight neonates. *Am. J. Obstet. Gynecol.* 214 380.e381-380.e386.

- Wellons 3rd, J.C., Shannon, C.N., Holubkov, R., Riva-Cambrin, J., Kulkarni, A.V., Limbrick Jr., D.D., et al., 2017. Shunting outcomes in posthemorrhagic hydrocephalus: results of a hydrocephalus clinical research network prospective cohort study. *J. Neurosurg. Pediatr.* 20, 19–29.
- Wu, D., Chang, L., Akazawa, K., Oishi, K., Skranes, J., Ernst, T., et al., 2017. Mapping the critical gestational age at birth that alters brain development in preterm-born infants using multi-modal MRI. *Neuroimage* 149, 33–43.
- Yuan, W., Deren, K.E., McAllister 2nd, J.P., Holland, S.K., Lindquist, D.M., Cancelliere, A., et al., 2010. Diffusion tensor imaging correlates with cytopathology in a rat model of neonatal hydrocephalus. *Cerebrospinal Fluid Res.* 7, 19.
- Yuan, W., McAllister 2nd, J.P., Lindquist, D.M., Gill, N., Holland, S.K., Henkel, D., et al., 2012. Diffusion tensor imaging of white matter injury in a rat model of infantile hydrocephalus. *Childs Nerv. Syst.* 28, 47–54.
- Yuan, W., McKinstry, R.C., Shimony, J.S., Altaye, M., Powell, S.K., Phillips, J.M., et al., 2013. Diffusion tensor imaging properties and neurobehavioral outcomes in children with hydrocephalus. *AJNR Am. J. Neuroradiol.* 34, 439–445.